
Revealing the Basis: Ordinal Embedding through Geometry

Jesse Anderton
 Northeastern University
 Boston, Massachusetts USA
 jesse@ccs.neu.edu

Virgil Pavlu
 Northeastern University
 Boston, Massachusetts USA
 vip@ccs.neu.edu

Javed Aslam
 Northeastern University
 Boston, Massachusetts USA
 jaa@ccs.neu.edu

Abstract

Ordinal Embedding places n objects into \mathbb{R}^d based on comparisons such as “ a is closer to b than c .” Current optimization-based approaches suffer from scalability problems and an abundance of low quality local optima. We instead consider a computational geometric approach based on selecting comparisons to discover points close to nearly-orthogonal “axes” and embed the whole set by their projections along each axis. We thus also estimate the dimensionality of the data. Our embeddings are of lower quality than the global optima of optimization-based approaches, but are more scalable computationally and more reliable than local optima often found via optimization. Our method uses $\Theta(nd \log n)$ comparisons and $\Theta(n^2 d^2)$ total operations, and can also be viewed as selecting constraints for an optimizer which, if successful, will produce an almost-perfect embedding for sufficiently dense datasets.

1 Introduction

Ordinal Geometry is a family of related problems that deals with a collection of objects which are presumed to lie in some metric space with an unknown metric. Unable to directly use features/positions, distances, or similarity scores, we instead attempt to either recover the metric (positions or distances), or to perform tasks such as clustering or classification, using only ordinal comparisons of the form, “Object a is closer to object b than to object c .”

For example, a collection of movies can be analyzed without extracting features by asking moviegoers questions like, “Is *Star Wars* more similar to

The Matrix or to *Star Trek*?” Similarly, one might analyze songs or musicians without having the musical expertise to design a feature representation for either by soliciting user preferences like, “If you love *The Rolling Stones*, you will prefer *Bruce Springsteen* to *Madonna*.” Similarity on food dishes might depend on factors like smell and taste, yet it’s not obvious how to obtain consistent features per dish; still, people have no trouble comparing foods.

These comparisons are commonly gathered from human assessors, who often find it easier to report on relative similarity than to provide explicit distances. In other cases, ordinal information can be inferred from known features as a regularization, dimensionality reduction, or representation learning technique. Ordinal Embedding, which seeks to recover the metric, has much in common with Metric/Kernel Learning but differs in that we generally have no underlying features.

In this paper we address the problem of recovering the object pairwise distances (or simply “recovering the metric”) using a minimum number of comparisons, assuming the underlying metric is Euclidean (i.e. the objects exist in an unknown Euclidean space) and that comparisons are always answered correctly. Note that recovering the full matrix of pairwise distances is mathematically equivalent to an embedding into a space isomorphic with the original data space up to scaling, rotation, reflection, and translation. With the metric in hand we can run standard machine learning tools, either by employing positions as vectors of latent features or by using the metric as a similarity kernel.

Problem Context. Jamieson and Nowak (2011) proved a lower bound of $\Omega(nd \log n)$ adaptively selected comparisons to fully recover the underlying metric space. While our work only fully recovers the metric for certain “ideal” datasets, it is the first published non-trivial algorithm with an upper bound matching the lower bound and thus establishes a performance baseline for future algorithms.

The theoretical results of Kleindessner and von

Luxburg (2014) and Arias-Castro (2015) prove that full metric recovery is possible given a total ordering of the k -nearest neighbors (k NN) of each point, when the dataset meets certain distributional requirements and for $k = \omega((n \log n)^{1/2})$, but do not propose an algorithm to do so. Hashimoto et al. (2015) provide an algorithm to fully recover the metric when $k = \omega(n^{2/(d+2)}(\log n)^{d/(d+2)})$, and which performs well even when $k = \log n$. The problem of comparison selection for full metric recovery is thus reduced to efficiently identifying the k NN of each point. However, we are not aware of any k NN algorithms using only $O(nd \log n)$ comparisons in the ordinal geometry setting. Despite the vast literature on identifying the k NN for a set, all the algorithms we have surveyed rely on known positions or distances.

The trivial way to obtain all possible comparisons is to sort all n points by increasing distance to each of the n possible “heads,” for $O(n^2 \log n)$ comparisons. Alternatively, a selection algorithm can be used to obtain all objects’ k NN using $O(n^2)$ comparisons. In either case, an embedding algorithm can then be used to (hopefully) recover the metric. When $d = \Omega(n)$, this is the best that can be accomplished.

The present work contains the first non-trivial upper bound on the problem when $d = o(n)$, matching the lower bound to (1) produce an embedding to recover the metric down to scaling for “ideal” datasets, and to (2) produce the input required for a high-quality embedding for many realistic “non-ideal” datasets. We also study the properties a dataset needs for our method to work well, showing where future work can generalize our approach to further classes of problems.

Most existing work on ordinal embedding, such as Soft Ordinal Embedding, or SOE (Terada and von Luxburg, 2014), focuses on optimizing a non-convex Machine Learning objective within a Euclidean space of some assumed dimensionality. We have empirically found that even when all comparisons are consistent with a Euclidean metric and the optimizer is given the correct dimensionality, optimization-based methods for ordinal embedding often struggle to find a global optimum or to deal with large datasets. We have also found that local optima tend to produce rankings that are nearly-random (when sorting by distance to any given object).

The present work takes on the challenges of state-of-the-art methods, namely scalability and reliability, by considering the underlying geometry of the problem, and avoiding optimization at some expense of performance. Our main contributions are:

- an algorithm to quickly produce embeddings of moderate to high quality using computational ge-

ometry rather than optimization;

- the first published algorithm to adaptively select a number of comparisons within a constant factor of the lower bound which achieves nearly-perfect embeddings for realistic datasets ($d \ll n$ and “not too sparse”); and
- the first published latent dimensionality estimator for ordinal datasets.

We also introduce subroutines which provide convex hull estimation, perpendicular line discovery, and a test of affine independence.

Our approach. We build our algorithm on the following intuition. Suppose that for some finite dataset $X \subset \mathbb{R}^d$ we also had access to d orthogonal “axes”, not as actual lines or segments, but in the form of d subsets of points A_1, \dots, A_d . The points on each axis are colinear, dense (max gap ϵ), and evenly-spaced. Additionally each A_i is “long enough” so that every point in X has a “projection” on it.

Each axis A_i contains two special “endpoints”; the A_i points have the *order-consistent property* that sorting by increasing distance from one endpoint is equivalent to sorting by decreasing distance from the other endpoint. For each point x in X , we can approximate its geometric projection to an axis A_i by locating the closest point on A_i to x with a binary search (using triplet comparisons), for a total cost of $\Theta(nd \log m)$ comparisons, where $m = \max_i |A_i|$. The coordinate is given by the rank of that closest axis point from an arbitrary endpoint. Note that if the axis points are evenly distributed, then each ordinal coordinate point is within ϵ of the (rescaled) true projection on that axis; if ϵ is small enough, this embedding recovers the original metric space with arbitrary precision.

Throughout the paper, we refer to such a set of points (A_i) as an “axis,” and to the collection of axes as a “basis.” In general, a real dataset will not contain evenly-spaced points along the axes of a perfect basis, but we achieve good performance with axis points which are only approximately collinear and axes which are only approximately orthogonal. We will show how to find such axes as subsets of X . The axes we find, as sets, have the order-consistent property between endpoints, so ranking is non-ambiguous. Other desirable properties for high quality ordinal coordinates are:

- (1) enough axes to account for differences between points,
- (2) axes that are closer to being orthogonal,
- (3) axes that extend to the boundaries of a bounding box for the set,
- (4) points along all axes that are evenly-spaced, and
- (5) gaps between points on each axis that are smaller than gaps between off-axis points.

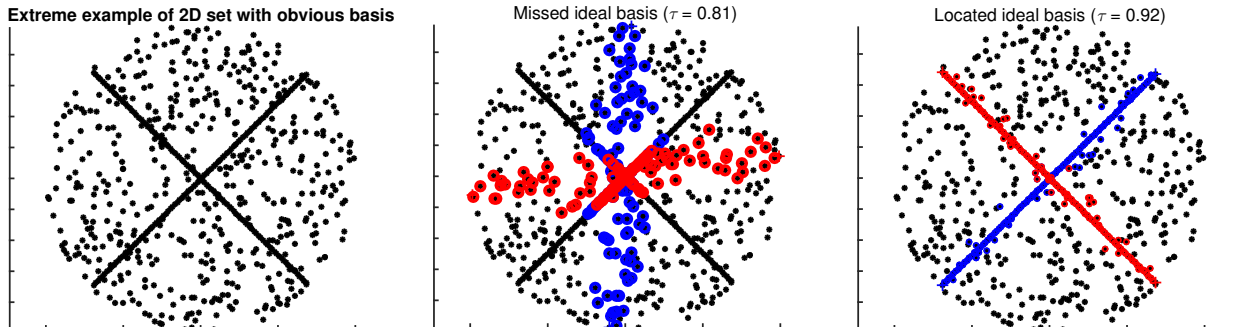


Figure 1: 2D points set X (left) includes two subsets of colinear, dense, evenly-spaced, points that make obvious long-enough axes. Middle: two axes red and blue found by our algorithm are not the best basis, but reasonable; τ is the mean Kendall’s τ between true rankings and basis-estimated rankings. Right: ideal axis red, blue also include few other points (criteria in Fig 2) since the gap on the colinear points is not small enough; thus $\tau < 1$.

Note that we do not require the axes to intersect (i.e. for $d > 2$ we do not need to have an origin point).

We address (1) through estimating affine independence, (2) through the symmetry of sphere intersections, and (3), roughly, through finding points close to the boundary of the convex hull of X (denoted $\text{conv}(X)$), but do not directly address (4) or (5) in the present work. For this reason, our method works best under relatively smooth density conditions and does not perform as well with high-dimensional datasets or datasets with rapidly-varying densities. See Figure 1 for the impact of missing the “ideal” basis.

If ϵ is the radius of the largest open ball in $\text{conv}(X)$ which contains no members of X , we say X is ϵ -dense. It is easy to show that as $\epsilon \rightarrow 0$ the basis our algorithm finds converges to a perfect basis and thus we fully recover the underlying metric. When our basis is imperfect, we can still use it to efficiently perform tasks such as finding the k -nearest neighbors of each member of X , or producing input to the user’s favorite embedding routine (such as SOE).

2 Finding an Approximate Basis

Algorithm 1 is our basis-finding algorithm. Each of the \hat{d} axes is formed by choosing pairs of endpoints near the boundary of X and finding points from X close to their (linear) convex hull. The first axis is formed using two points opposite each other on the boundary of $\text{conv}(X)$, using that the most-distant point from any member of X is on this boundary. After that, we find new axes which are likely to be orthogonal to the previous set of axes by identifying points which are far from the convex hull of the previous axis endpoints (see Section 2.1). In our algorithm, $r_{p_i}[\cdot]$ returned by `SortForHead`(p_i, oracle) is the array of the ranks of all objects $x \in X$ sorted by distance from endpoint p_i .

We fully describe our algorithm in the following sub-

sections, and analyze its cost here. Line 2 uses $n - 2$ comparisons. Each call to `SortForHead` sorts all objects in $\Theta(n \log n)$ comparisons. We make two calls per axis, so we use $\Theta(n\hat{d} \log n)$ comparisons (within the theoretical bound as long as $\hat{d} = O(d)$).

The $\widehat{\text{conv}}$ function (Eq. 3) estimates the convex hull of a set of points based on their rankings of the other points. It uses $O(n^2\hat{d})$ operations (not comparisons), because it has to iterate over all $2^{\hat{d}}$ rankings for each point. The calculation on Line 12 to find the next candidate takes $O(n\hat{d})$ operations to scan the axis endpoints’ rankings of each point in X . Thus, `ChooseBasis` uses $\Theta(n^2\hat{d}^2)$ total operations.

2.1 Choosing Axes

We identify axes by choosing axis endpoints which are as far as possible from the convex hull of the previous axis endpoints. Let $P = \{p_1, \dots, p_{2\hat{d}}\}$ be the set of endpoints for the \hat{d} axes found so far. A straightforward approach, different than ours, is a *farthest-rank-first traversal of X* (FRFT) adapted from Gonzalez (1985): choose endpoints as far as possible (in rank) from the previous axis endpoints, i.e. by $\text{argmax}_{x \in X} \{\min_{p \in P} r_p[x]\}$.

This forms a rank-based approximation of an ϵ -net, which can be used to approximate the geometric distribution of a set of points. The axis endpoints thus found are well-separated from each other, and tend to lie closer to regions of higher density than the points of an ϵ -net. However, our testing occasionally found that some of the resulting axes are nearly parallel.

We present a more reliable approach. We first discuss the notions of a *lens* and its *apex*, and *aboveness*. Suppose we have selected a single axis with endpoints p_1 and p_2 , and that for all $x \in X$ we find that $d(p_1, x) \leq d(p_1, p_2)$ and $d(p_2, x) \leq d(p_2, p_1)$. Then the set X lies within the *lens* between p_1 and p_2 — the

Algorithm 1: ChooseBasis($n, oracle$)

Input : n is the number of objects in the collection
 $oracle(a, b, c)$ decides whether b or c is
 closer to a .

Output: A basis $(A_1, \dots, A_{\hat{d}})$, where each axis A_i
 lists points near a line crossing the dataset.

```

1  $z \leftarrow$  a randomly selected point ;
2  $p \leftarrow$  furthest point from  $z$  ; // first axis endpoint
3  $r_p[\cdot] \leftarrow$  SortForHead( $p, oracle$ ) ;
4  $P \leftarrow \{p\}$  ;
5 for  $i \leftarrow 1, 3, 5, \dots, n$  do
    // Complete the  $(i+1)/2$  axis
6    $p_i \leftarrow p$  ;
7    $L \leftarrow \{x : r_{p_j}[x] \leq r_{p_i}[x], \forall j < i\}$  ; // Lens
8    $p_{i+1} \leftarrow \operatorname{argmax}_{x \in L} r_{p_i}[x]$  ; // Apex oppos.  $p_i$ 
9    $r_{p_{i+1}}[\cdot] \leftarrow$  SortForHead( $p_{i+1}, oracle$ ) ;
10   $\hat{d} \leftarrow (i+1)/2$  ;
11   $A_{\hat{d}} \leftarrow \widehat{\operatorname{conv}}(\{p_i, p_{i+1}\})$  ;
    // Verify candidate for next axis
12   $p \leftarrow$  point "above" max # of points in  $\widehat{\operatorname{conv}}(P)$ ;
13  if no point is "above" any other then
14    | break;
15   $r_p[\cdot] \leftarrow$  SortForHead( $p, oracle$ ) ;
16   $P \leftarrow P \cup \{p\}$  ;
17  if  $\hat{d} = 1$  then
18    |  $P \leftarrow P \cup \{p_{i+1}\}$  ;
    // Test affine independence
19  if  $\widehat{\operatorname{conv}}(P) = \cup_{z \in P} \widehat{\operatorname{conv}}(P \setminus \{z\})$  then
20    | break;
21 return  $(A_1, \dots, A_{\hat{d}})$  ;
    
```

intersection of the closed balls centered on p_1 and p_2 with radii both equal to $d(p_1, p_2)$. Future ideal axis endpoints will lie close to the *apex* of this lens: the set of points $\mathcal{A}(\{p_1, p_2\})$, where

$$\mathcal{A}(P) \equiv \{x \in \mathbb{R}^d : \forall p \in P, d(x, p) = \max_{q \in P} d(p, q)\} \quad (1)$$

is the intersection of the (hollow) spheres centered on vertexes P that surround P . In general on d dimensions, d points will create an apex of 2 points, $d-1$ points an apex of a circle, $d-2$ points a sphere, etc. A "lens" can similarly be formed by choosing a point $a \in X$ as an apex and using the distances $d(p, a)$ for each $p \in P$ as the ball radii ("lens" is informal here, as it is the intersection of $|P|$ and not strictly 2 balls).

When points near the lens apex exist in X , these points are ideal choices because they are as far as possible from, and form orthogonal lines to, the line between p_1 and p_2 . FRFT will naturally choose these points, when possible. However, these points only exist in X when the range along all dimensions is almost equal.

We say that point p is *above* point q with respect to

some set P if for all $a \in P$ we have $d(a, p) > d(a, q)$. See Figure 2 for an example. This means that q lies in the "lens" of P with p as its apex. By Theorem 3 below, p can thus not be in $\operatorname{conv}(P)$. If the set P is fixed, above-ness is transitive: if p is above q and q is above z , that implies p is above z .

Point p is above q , with respect to p_1, p_2

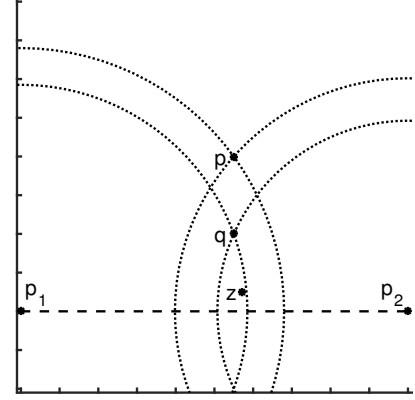


Figure 2: Point p is "above" q because q is found in the intersection of balls centered on p_1 and p_2 and extending to p . This implies that p is farther from the line than q and thus not in $\operatorname{conv}(\{p_1, p_2\})$.

Axis endpoints selection. The first new axis endpoint $p_i = p$ (Algorithm 1 line 12) is chosen to be above a maximal number of points in the convex hull of prior endpoints. If there is a point close to the apex of the ball intersection, it will be above nearly the entire set and will be chosen as the maximum (and our algorithm will make the same choice as FRFT). If there is no such point then we will choose a point which is above as many points as possible, hoping for a point above a dense region of X which also lies close to the apex of the ball intersection. The second point p_{i+1} (line 8) is chosen to approximate the apex opposite the first endpoint p_i in the lens with p_i as an apex.

Dimensionality estimate \hat{d} . We stop adding axes as soon as our next axis endpoint p does not appear to be affinely-independent of the previous axis endpoints. Our test for affine independence relies on Carathéodory's Theorem, which states that any point in the convex hull of a set of points in \mathbb{R}^d can be expressed as a convex combination of just $d+1$ or fewer of them. We define a set P containing both endpoints for the first axis, plus the first endpoint of each additional axis and our new candidate p . We have $|P| = \hat{d} + 2$. Suppose we have already found d dimensions, and the new axis endpoint is simply not in the convex hull of the previous endpoints. Then any point in $\operatorname{conv}(P)$ is also in the convex hull of some set of all but one of the points in P . On the other hand, if $d > \hat{d}$ then these extra hulls are the faces of a higher-dimensional

Table 1: Dimensionality Estimates
 (1,000 points, avg. of 100 runs)

True d :	1	2	3	5	8	10	20
Ball	1	2	2.11	3.66	4.22	4.54	5.53
Cube	1	2	2.37	3.74	4.44	4.58	4.78
Gaussian	1	2	2.98	3.91	4.44	4.54	4.52
Sphere	1	1	2	3.09	3.85	4.08	4.93

manifold, and we expect some of the points in that manifold to be far enough from the convex hulls to not be included in our \widehat{conv} estimates.

We prove that our dimensionality estimate \hat{d} is always at most the true dimensionality d and that it converges to d as $\epsilon \rightarrow 0$ in Theorem 4 in Appendix A.4. See Table 1 for dimensionality estimates on various datasets. Since the number of points in each dataset is the same, as the dimensionality increases the density constant ϵ grows. This causes \widehat{conv} to be less precise and leads us to underestimate the dimensionality.

2.2 Convex Hull Estimation

Our convex hull estimation \widehat{conv} works because any union of balls which all coincide in some point must contain the convex hull of the ball centers. We prove this as Theorem 3 in Appendix A.1.

Suppose we want to identify points from X which lie in the convex hull of a set $P = \{p_1, \dots, p_k\} \subset X$. The intersection of X and such a union of balls can easily be formed by choosing some point q and taking the set

$$C_q(P) \equiv \{x \in X : \exists p \in P, r_p[x] \leq r_p[q]\}. \quad (2)$$

In order to reduce false positives, we take the intersection of C_q across all possible points q as our estimate.

$$\begin{aligned} \widehat{conv}(P) &= \bigcap_{q \in X} C_q(P) \\ &= \{x \in X : \forall q \in X, \exists p \in P, r_p[x] \leq r_p[q]\} \end{aligned} \quad (3)$$

As the intersection of sets containing $conv(P) \cap X$, we know $\widehat{conv}(P)$ contains $conv(P) \cap X$. Theorem 1, proved in Appendix A.2, says that any false positives in our estimate are close to the boundary of $conv(P)$. See Figure 3 for an example of an axis we might select.

Theorem 1. *Let $\widehat{conv}(A)$ be the estimate of $conv(A)$ for some $A \subseteq X \subset \mathbb{R}^d$. If the largest empty ball in $conv(\widehat{conv}(A))$ has radius ϵ , and the maximum distance between any two points in A is m , then for any $c \in \widehat{conv}(A)$ the distance to the closest point $c' \in conv(A)$ is less than $\sqrt{\epsilon(2m + \epsilon)}$. Further, there is no point $x \in X$ such that $r_a[x] < r_a[c]$ for all $a \in A$.*

It is easy to show that the points in any axis are order-consistent: increasing distance order from one axis

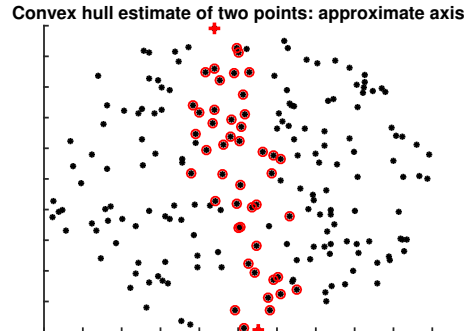


Figure 3: Red points are within \widehat{conv} of the two (blue) endpoints. Although some of these points are very close together, none is “above” any other w.r.t. the endpoints. Lenses are very thin near the line.

endpoint is decreasing distance order from the other endpoint (matching the intuition for points along a line). However, the points may be somewhat distant from the line in an arbitrary direction.

2.3 Embedding Each Point

Given an approximate basis $A_1, \dots, A_{\hat{d}}$, the next step is to embed the points within the basis. We accomplish this without any additional comparisons.

Ideally, along each axis A_i the points would be evenly-spaced and lie along the line between the axis endpoints. We could then embed any $x \in X$ by simply finding the index of the closest point via binary search, since the members of A_i would be sorted as a bitonic array: the distance to x would descend to a minimum and then ascend. The total comparisons cost would be $O(n \hat{d} \log n)$ (within the theoretical bound).

In practice, we never have such perfect axes. When the points of X are in general position, no member of X will be found in the convex hull of any subset of d or fewer points and no member of A_i except the endpoints will lie on the line. A binary search will not find the closest point in A_i to x because the points will not be exactly sorted by distance to x . Further, the closest point in A_i will often be closest simply because it is not found on the endpoints-line, not because it is near the projection x' of x onto the line (Figure 4).

We really want to find the point in A_i which is closest to x' , not closest to x . The projection x' will be in the center of the lens formed from the axis endpoints with x at its apex. The lens will always contain some member of A_i (otherwise $x \in A_i$). We select as the ordinal coordinate of x along A_i the **median index** for those axis points inside this lens.

While this may not be the point in A_i closest to x' , especially if the density varies greatly along A_i , it costs no additional comparisons to select this point.

We guess that location 5 is closest to x'

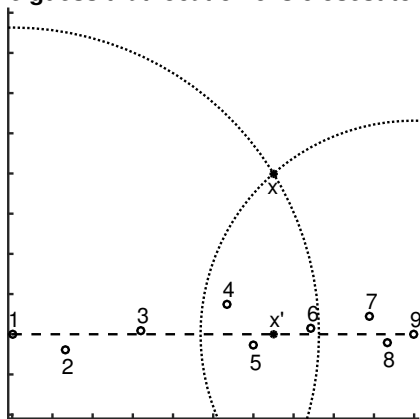


Figure 4: The circled points are members of axis A_i . We choose the median point within the lens beneath x (containing 4, 5, and 6) as our guess at the closest point to its projection, x' .

We have found that the empirical performance on our datasets is comparable to finding the point in the lens closest to x through a linear search.

While even in dense spaces our algorithm might not find orthogonal axes, if the discovered axes are indeed orthogonal we can guarantee that our embedding recovers the original metric with a precision depending on the density of X and the true dimensionality.

Theorem 2. *If any ball of radius ϵ in $\text{conv}(X)$ contains at least 1 and at most k points, and assuming $\hat{d} = d$ orthogonal axes are found which extend to the faces of a bounding box for X , using linear search in the lens for points' coordinates, then there is a scaling constant $s \in \mathbb{R}$ such that for any two points $x, y \in X$,*

- the coordinate x_i on any axis A_i is bounded by its projection x'_i by $(s/k)x_i - \epsilon \leq x'_i \leq sx_i + \epsilon$, and
- the scaled distance estimate $\hat{d} := s \cdot \widehat{\text{dist}}(x, y)$ is within $2k\epsilon\sqrt{d}$ of the true distance, i.e., $\text{dist}(x, y) - 2\epsilon\sqrt{d} \leq \hat{d} \leq k(\text{dist}(x, y) + 2\epsilon\sqrt{d})$.

This is proven in the appendix. If we fix d and the diameter of X in each dimension, assuming orthogonal axes, this theorem implies that when $\epsilon \rightarrow 0$ the value of $|X|$ approaches infinity and the distances are recovered, down to scaling, recovering the original metric.

3 Basis Evaluation Results

We show here that our algorithm produces good embeddings on real datasets, and that an optimization-based embedding of our triples often yields an even better result.

Datasets. We evaluate against several generated and real datasets. In an attempt to fully exercise

our algorithm, we include some datasets which are not well-suited to it. We answer all similarity questions based on Euclidean distances between the original features/positions. The `3dggmm`, `5dggmm`, and `5dcube` datasets are random draws of 500 points from Gaussian mixtures and the unit cube.

For `cities`, we select 500 cities by choosing the most populous city in each country and then additional cities from most to least populous. Cities are represented in Euclidean coordinates converted from their latitudes and longitudes. We use continents as class labels. All cities lie on the convex hull, so ϵ is the diameter of the set. This leads to a smaller dimensionality estimate and somewhat worse performance.

We use 1,000 records from `MNIST Digits`, treating raw pixel values as 784 features. `Digits` roughly consists of clusters of points around class labels, with gaps between them. We thus have a fairly large ϵ , and wildly varying density across the dataset. We also take 1,000 records from `Spambase` with 57 features. Performance on `spambase` is especially strong. Our basis for this dataset outperforms all the others, although SOE was not able to find a global optimum from our triples.

Finally, we take 2000 records from `20newsgroups`, using TF-IDF scores for 34,072 terms as features. These records are modified using the `scikit-learn` Python package to remove headers, footers, and quotes, and we only select records having at least 50 nonzero feature values. This dataset has $d \gg n$ and very sparse feature vectors. This type of distribution is ill-suited to our algorithm, and performs the worst.

Evaluation. We evaluate by comparing all rankings or distances between an embedding and the original dataset. We report mean Kendall's τ , mean k NN precision for $k = \lceil \log_2 n \rceil$, and distance RMSE.

Distance RMSE (root mean squared error), is based on the fact that in a perfect embedding all pairwise distances would be scaled by the same constant. Recall that $d(x, y)$ is the distance between x and y in X , and denote the distance in some embedding \hat{X} by $\hat{d}(x, y)$. If \hat{X} recovers X , then there is some $s \in \mathbb{R}$ such that for all points $x, y \in X$, $d(x, y) \approx s\hat{d}(x, y)$. We fit an optimal s and report the RMSE of the residuals,

$$\text{rmse}(X, \hat{X}) \equiv \min_s \left(\frac{1}{n} \sum_{i < j} (d(x_i, x_j) - s\hat{d}(x_i, x_j))^2 \right)^{1/2}$$

Smaller is better and zero is perfect, but the numbers are not comparable across different datasets.

Experiments. Our results are in Table 2. **Basis** is the embedding our geometric algorithm produces.

Table 2: Embedding Quality

* indicates global optimum was not found; means procedure computationally too expensive

Method	Dataset	d	\hat{d}	# Cmp.	τ	knn	rmse	Method	Dataset	d	\hat{d}	# Cmp.	τ	knn	rmse
Basis	3dgm	3	3	38K	0.71	0.64	0.77	Basis	20news	34K	3	186K	0.11	0.06	0.53
Basis+SOE	3dgm	3	3	38K	0.99	0.97	0.02	Basis+SOE	20news*	34K	6	186K	0.01	0.01	0.34
Extra+SOE	3dgm	3	3	61K	0.99	0.99	0.01	Extra+SOE	20news*	34K	6	310K	-0.01	0.01	0.34
Rand+SOE	3dgm	3	3	38K	0.95	0.81	0.11	Rand+SOE	20news*	34K	3	186K	0.01	0.01	0.44
CK	3dgm*	3	3	38K	-0.01	0.02	1.79	CK	20news	34K	16	—	—	—	—
Basis	5dcube	5	3	39K	0.49	0.40	0.26	Basis	cities	3	2	28K	0.37	0.35	0.60
Basis+SOE	5dcube	5	6	39K	0.88	0.73	0.05	Basis+SOE	cities	3	4	28K	0.89	0.54	0.13
Extra+SOE	5dcube	5	6	61K	0.94	0.92	0.03	Extra+SOE	cities	3	4	50K	0.96	0.93	0.05
Rand+SOE	5dcube*	5	6	39K	0.61	0.30	0.19	Rand+SOE	cities*	3	4	28K	0.01	0.02	0.75
CK	5dcube*	5	5	39K	0.01	0.02	0.34	CK	cities*	3	3	28K	0.01	0.02	0.67
Basis	5dgm	5	3	39K	0.68	0.60	0.90	Basis	digits	784	6	159K	0.52	0.29	3.18
Basis+SOE	5dgm	5	6	39K	0.94	0.66	0.14	Basis+SOE	digits*	784	12	159K	0.01	0.01	2.48
Extra+SOE	5dgm	5	6	62K	0.98	0.97	0.04	Extra+SOE	digits*	784	12	211K	0.01	0.01	2.49
Rand+SOE	5dgm*	5	6	39K	0.01	0.02	1.77	Rand+SOE	digits*	784	12	159K	0.73	0.40	2.31
CK	5dgm*	5	5	39K	-0.01	0.02	1.57	CK	digits	784	10	—	—	—	—
Basis	spam	57	3	85K	0.85	0.78	471	Basis	spam	57	3	85K	0.85	0.78	471
Basis+SOE	spam*	57	6	85K	-0.01	0.01	596	Basis+SOE	spam*	57	6	85K	-0.01	0.01	596
Extra+SOE	spam*	57	6	138K	0.01	0.01	596	Extra+SOE	spam*	57	6	138K	0.01	0.01	596
Rand+SOE	spam	57	3	85K	0.94	0.23	150	Rand+SOE	spam	57	3	85K	0.94	0.23	150
CK	spam	57	10	—	—	—	—	CK	spam	57	10	—	—	—	—

Basis+SOE uses the triples collected by **Basis** as input to the Soft Ordinal Embedding (SOE) algorithm (Terada and von Luxburg, 2014). **Extra+SOE** runs use additional comparisons to improve the embedding as described in Section 4.

SOE does very well when a global optimum is found, but often takes many random initializations to find one. We attempt 20 embeddings in \hat{d} dimensions; if the minimal loss is above 10^{-3} , we try again in $2\hat{d}$ dimensions and report the best of 20 embeddings in the higher dimensionality. Even a small amount of loss from the SOE objective can lead to a poor embedding, and for several of our datasets it was simply unable to find a global optimum or even a competitive local optimum (at least, not in 40 attempts). Note that zero loss is always possible for correct comparisons in the true dimensionality, but not necessarily in \hat{d} dimensions. In general, one never knows whether a particular loss threshold can be achieved, especially given noisy or potentially non-Euclidean comparisons.

Baselines. We compare against two baselines. Notably, **Basis** is much faster than the baselines, completing in less than two seconds for each dataset and often much less than one. In contrast, the SOE runs took more than 24 hours to repeat embeddings with new random initializations, and the CK runs took several days to generate triples.

Rand+SOE picks random comparisons in round robin style for each head until its budget is exhausted, and

Table 3: Classification Accuracy, 5 folds

Dataset	d	Original		Embedding		
		Train	Test	\hat{d}	Train	Test
20news	34K	0.94	0.54	3	0.21	0.08
cities	3	1	0.95	2	0.99	0.90
digits	784	1	0.84	6	0.92	0.71
spam	57	0.99	0.97	3	0.85	0.74

then embeds them with SOE. SOE generally struggled to embed these triples, but performance was good when it worked. **CK** runs the CrowdKernel method (Tamuz et al., 2011) up to the number of triples used to build our basis, and evaluates the resulting CrowdKernel embedding. We used the authors’ CrowdKernel code, but it was not able to handle the larger datasets. We report all datasets which completed.

As a simple test of downstream utility, we trained Gradient Boosting classifiers on our basis embeddings and compared the classification accuracy to classifiers trained on the original feature space. The results can be seen in Table 3. Performance is good even with $\hat{d} \ll d$, with the exception of the ill-suited **20newsgroups** (which is at least better than random).

4 Improving the Ordinal Embedding

Once we have obtained an embedding of reasonably high quality, it is not difficult to adaptively select new triples to drive the quality upward. First, we pause

to consider the information that can already be inferred from the triples gathered thus far. Any geometric properties implied by the triples must be true of any embedding that satisfies them, so this helps us reason about what we have already “told” the optimizer.

We have sorted all points from the endpoints of each axis, and selected endpoints that are near the boundaries of the set. This already carries a lot of information to an embedding algorithm. The estimates \widehat{conv} are fixed for any subset of axis endpoints, establishing a layer of points near their hulls. We know the set of points which are only “above” points in \widehat{conv} , establishing a second layer, and we similarly know the contents of every layer up to the set boundary.

We lack information about dimensions whose extents were too small or sparse for us to discover. We don’t know exact distances, so we can’t immediately identify the k -nearest neighbors of each point. With the results of Terada and von Luxburg (2014) and Hashimoto et al. (2015) in mind, showing good performance embedding based on the k NN with $k = \log n$, we sort the $2k$ nearest points to each point within our embedding, costing $\Theta(nk \log k)$ additional comparisons. For our experiments, we use $k = \log_2 n$ for a total cost of $\Theta(n \log n \log \log n)$ additional triples. Note that if you wish to simply identify the k NN rather than sort them, a selection algorithm can instead be used for $\Theta(n \log n)$ new comparisons in total, staying within the lower bound. The result is in Table 2 as the **Extra+SOE** line. In all cases, the embedding quality improved.

5 Related Work

Ordinal Embedding, a.k.a. non-metric embedding or non-metric multidimensional scaling, has been studied for over sixty years. Optimal comparison selection, however, is less studied. When all answers are known in advance (i.e. from features), practitioners either use them all, select a random subset, identify the k NN, or sort a set of “landmark” objects. Jamieson and Nowak (2011) suggest using embeddings to determine whether a question can be decided from prior answers. The only adaptive algorithm we have found which works in practice is the CrowdKernel algorithm by Tamuz et al. (2011). Given an intermediate embedding based on prior answers, it greedily selects new questions for each object to maximize the expected information gain for the embedding objective. This method outperforms random selection (apparently by selecting tails closer than average to the head), but its embeddings compare poorly to those of Soft Ordinal Embedding.

Ordinal embedding has been heavily studied, particularly by the metric and kernel learning communities. Early approaches employed semidefinite programming

(Weinberger et al., 2006; Xing et al., 2003) and/or required eigenvalue decompositions. Later approaches focused on minimizing Bregman divergences (Davis et al., 2007; Kulis et al., 2009; Jain et al., 2012), which is guaranteed to find a positive semidefinite (PSD) kernel, or on ignoring semidefiniteness until convergence and projecting the output matrix to the nearest PSD matrix (Chechik et al., 2010). Ordinal embedding without features has also been studied by Agarwal et al. (2007, 2010), who provide a flexible and modular algorithm with proven convergence guarantees. McFee and Lanckriet (2011) considers how to learn a similarity function which is as consistent as possible with multiple feature sets as well as ordinal constraints. Local (and Soft) Ordinal Embedding (Terada and von Luxburg, 2014) recovers the metric with guarantees on accurate density recovery. Hashimoto et al. (2015) prove metric recovery over certain directed graphs, of including k NN adjacency graphs.

Our algorithm relies on a sort routine, so when an unreliable oracle is used it is natural to consider the deep literature on crowdsourcing sort algorithms (Marcus et al., 2011; Niu et al., 2015) and on noise-tolerant sorting (Ajtai et al., 2009; Braverman and Mossel, 2008; Hadjicostas and Lakshmanan, 2011).

6 Conclusion and Future Work

We have presented a Computational Geometric approach to Ordinal Embedding which offers new theoretical insights into the problem. In particular, we have contributed approximate algorithms for dimensionality estimation, tests of convex hull membership and affine independence, and perpendicular line discovery. We have combined these methods to find an approximate basis within which points can easily be positioned. When run on a sufficiently dense set of relatively low dimensionality, we can reliably and efficiently produce a medium-to-high quality embedding. When an optimizer finds a global optimum for our triples, the user obtains a high quality embedding.

While we have not “solved” the embedding or triple selection problems and do not suggest replacing optimization approaches entirely, our approach provides new insights into the geometric information contained in a set of triples and we believe it will lead to faster and more reliable future approaches.

References

- Arvind Agarwal, Jeff M. Phillips, and Suresh Venkatasubramanian. Universal multi-dimensional scaling. *SIGKDD*, 2010. doi: 10.1145/1835804.1835948.
- Sameer Agarwal, Josh Wills, Lawrence Cayton, Gert Lanckriet, David Kriegman, and Serge Belongie. Generalized non-metric multidimensional scaling. *AISTATS*, 2007.
- Miklós Ajtai, Vitaly Feldman, Avinatan Hassidim, and Jelani Nelson. Sorting and Selection with Imprecise Comparisons. *ICALP*, 2009.
- Ery Arias-Castro. Some theory for ordinal embedding. *arXiv.org*, January 2015.
- Mark Braverman and Elchanan Mossel. Noisy sorting without resampling. *SODA*, 2008.
- Gal Chechik, Varun Sharma, Uri Shalit, and Samy Bengio. Large scale online learning of image similarity through ranking. *JMLR*, 2010.
- Jason V. Davis, Brian Kulis, Prateek Jain, Suvrit Sra, and Inderjit S. Dhillon. Information-theoretic metric learning. *ICML*, 2007.
- Teofilo F Gonzalez. Clustering to minimize the maximum intercluster distance. *Theoretical Computer Science*, 38:293–306, 1985.
- Petros Hadjicostas and K B Lakshmanan. Recursive merge sort with erroneous comparisons. *Discrete Applied Mathematics*, 159(14):1398–1417, August 2011.
- T B Hashimoto, Y Sun, and T S Jaakkola. Metric recovery from directed unweighted graphs. *AISTATS*, 2015.
- Prateek Jain, Brian Kulis, Jason V. Davis, and Inderjit S. Dhillon. Metric and kernel learning using a linear transformation. *JMLR*, 2012.
- Kevin G Jamieson and Robert D Nowak. Low-dimensional embedding using adaptively selected ordinal data. *49th Annual Allerton Conference on Communication, Control, and Computing*, 2011. doi: 10.1109/Allerton.2011.6120287.
- M Kleindessner and U von Luxburg. Uniqueness of Ordinal Embedding. *COLT*, 2014.
- Brian Kulis, Máttyás A. Sustik, and Inderjit S. Dhillon. Low-rank kernel learning with bregman matrix divergences. *JMLR*, 2009.
- Adam Marcus, Eugene Wu, David Karger, Samuel Madden, and Robert Miller. Human-powered sorts and joins. *Proc. VLDB Endow.*, 2011.
- Brian McFee and Gert Lanckriet. Learning Multimodal Similarity. *JMLR*, 12, February 2011.
- Shuzi Niu, Yanyan Lan, Jiafeng Guo, Xueqi Cheng, Lei Yu, and Guoping Long. Listwise Approach for Rank Aggregation in Crowdsourcing. *WSDM*, 2015.
- Omer Tamuz, Ce Liu, Serge Belongie, Ohad Shamir, and Adam Tauman Kalai. Adaptively Learning the Crowd Kernel. *arXiv.org*, May 2011.
- Yoshikazu Terada and Ulrike von Luxburg. Local ordinal embedding. *ICML*, 2014.
- Kilian Q. Weinberger, John Blitzer, and Lawrence K. Saul. Distance metric learning for large margin nearest neighbor classification. *NIPS*, 2006.
- Eric P. Xing, Andrew Y. Ng, Michael I. Jordan, and Stuart Russell. Distance metric learning, with application to clustering with side-information. *NIPS*, 2003.

A Proofs

In the following proofs, we use $B(c, r)$ to denote a closed ball in Euclidean space with center c and radius r , and $\text{conv}(x_1, \dots, x_k)$ to denote the convex hull (the set of all convex combinations) of points x_1, \dots, x_k . We also use $d(x, y)$ to denote the Euclidean distance between points x and y .

A.1 Convex Rankings

The proofs in this section show that our approximate convex hull contains all points from the convex hull, and that any extra points are not too far from the hull's boundary. We essentially show that for any point p outside the convex hull of a set V of points, there is some point q inside the convex hull which is closer to all the members of V than is p .

We first prove a useful lemma.

Lemma 1. *Let $V = \{v_1, \dots, v_k\}$ be an arbitrary set of points in Euclidean space, and p an arbitrary point not found inside $\text{conv}(V)$. There is a point $q \in \text{conv}(V)$ such that for all $v \in V$, $d(v, q) < d(v, p)$.*

Proof. Let $C := \text{conv}(V)$. Because C is convex, there is some unique point $q \in C$ which is closer to p than any other point in C , so for any arbitrary vertex $v \in V$ we have $d(p, v) \geq d(p, q)$. Since C is convex and q is the closest point in C to p , there is a hyperplane passing through q perpendicular to line pq which separates C from p . Thus, we must have either $q = v$ or $\angle pqv \geq 90^\circ$. So edge vp is the longest in $\triangle vpq$ and q is closer to v than is p . \square

Next, we show that any union of balls which all have at least one point in common will cover the convex hull of the ball centers. For example, for an arbitrary subset $V \subseteq X \subset \mathbb{R}^d$, the set of all points from X which are ranked no farther from the members of V than some common point p will contain all the points in $\text{conv}(V) \cap X$.

We next prove Theorem 3.

Theorem 3. *Let $\mathcal{B} = \{B(v_1, r_1), \dots, B(v_k, r_k)\}$ be a set of closed balls in \mathbb{R}^d with centers v_1, \dots, v_k and radii r_1, \dots, r_k , respectively. If all the balls in \mathcal{B} have at least one point in common, then $\text{conv}(\{v_1, \dots, v_k\})$ is a subset of their union.*

Proof. Let $B := \cup_i B(v_i, r_i)$, let $C := \text{conv}(v_1, \dots, v_k)$, and let q be an arbitrary point in C . We will prove that q is in at least one of the component balls in B . By Carathéodory's Theorem, there is some subset of at most $d + 1$ centers v_1, \dots, v_{d+1} (reabeled without

loss of generality) such that $q \in \text{conv}(v_1, \dots, v_{d+1})$. Let $C' = \text{conv}(v_1, \dots, v_{d+1}) \subseteq C$.

By Lemma 1, there is some point p contained in each of the $d + 1$ balls which is in C' . We can partition C' into $d + 1$ closed convex subsets by replacing each of its vertices v_i in turn with p . These subsets are d -simplexes with d ball centers and p as their $d + 1$ vertices. Observe that q must fall into one of these subsets (or more, if it falls on a boundary). Let P be one such d -simplex containing q , and let F be the face of the simplex formed by the d ball centers. Since q lies in P , another simplex Q can be formed using the same face F but with apex q instead of p . Call the heights of simplexes P and Q the distances from points p and q to their respective closest points in F , and observe that the height of Q is no greater than the height of P . Since $Q \subseteq P$, they share the same face F , and the height of Q is less than or equal to the height of P , there must be some vertex v_i of F such that $d(v_i, q) \leq d(v_i, p)$. Thus, any $q \in C$ is contained in B . \square

The following corollary provides a necessary condition for points in the convex hull of a set which we use for convex hull estimation.

Corollary 1 (convex hull rankings). *Let $V = \{v_1, \dots, v_k\}$ be an arbitrary set of points in Euclidean space, and let points p and q be arbitrary points in $\text{conv}(V)$. Then there is some $v \in V$ such that $d(v, p) \leq d(v, q)$.*

Proof. By Theorem 3, the union of balls centered on the members of V whose radii extend to q contain $\text{conv}(V)$. Since p is inside $\text{conv}(V)$, it must be within at least one of these balls. \square

A.2 Convex Hull Estimation

Given an arbitrary set of points $X \subset \mathbb{R}^d$ and any subset $V \subset X$, we can use Theorem 3 to identify members of X which are close to $\text{conv}(V)$ in the sense that they are either in $\text{conv}(V)$ or close to the boundary of $\text{conv}(V)$.

For any point $x \in X$, define the set $C(x) := \cup_{v \in V} \{y \in X : d(v, y) \leq d(v, x)\}$ as an estimate of the convex hull of V . By Theorem 3, $C(x) \subseteq \text{conv}(V)$. However, any individual estimate $C(x)$ will tend to contain many false positives. We can form a better estimate $\hat{C} := \cap_{x \in X} C(x)$. The following theorem shows that the false positives of this estimate contain only points which are close to the boundary of $\text{conv}(V)$.

We now prove Theorem 1.

Proof. By construction, for any points $c \in \hat{C}$ and $x \in$

X there is a vertex $v \in V$ such that $d(v, c) \leq d(v, x)$. However, by Lemma 1 we know that there are points in $\text{conv}(V)$ which are closer to any $v \in V$ than any member of \hat{C} which is not in $\text{conv}(V)$. Any point in \hat{C} which is not in $\text{conv}(V)$ is there because none of these points is contained in X .

Let $p \in \hat{C}$ be an arbitrary false positive, not contained in $\text{conv}(V)$, and let q be the closest point in $\text{conv}(V)$ to p . Note that since $q \notin X$, we know that q is not a member of V . This means that we tend not to make mistakes “close to the corners” of $\text{conv}(V)$.

For any vertex $v \in V$ let $r_v := d(v, p)$ be its distance to p . Define the set of points closer to all members of V than p as

$$E_p \equiv \bigcap_{v \in V} B(v, r_v). \quad (5)$$

We know E_p contains no members of X because p is a false positive. Since E_p is an intersection of balls, when $d(p, q)$ is greater all the radii r_v are also greater and the size of E_p is greater in all dimensions.

If $d(p, q)$ was sufficiently large, E_p would contain a ball of radius ϵ and would thus contain a member of X , forming a contradiction. The remainder of the proof establishes an upper bound on $d(p, q)$ under the assumption that an ϵ -ball centered at q is not contained in E_p . Refer to Figure 5 for a diagram of the following argument.

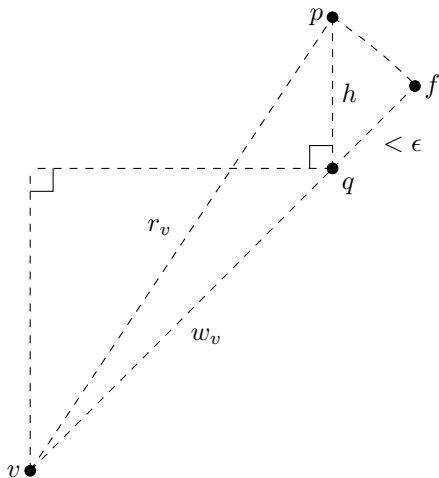


Figure 5: Our construction for Theorem 1. We want to maximize h such that $d(q, f) < \epsilon$. $v \in V$ is a convex hull vertex, and $p \in \hat{C}$ a false positive. q is the closest point in $\text{conv}(V)$ to p , and point f is collinear with vq . We have $h = d(p, q)$, $r_v = d(v, p) = d(v, f)$, and $z = d(v, q)$. By assumption, $d(q, f) < \epsilon$. Note that sometimes v and f are on the same face of $\text{conv}(V)$ as q , implying that $w = z$.

Let $v \in V$ be an arbitrary vertex, not necessarily on

the same face of $\text{conv}(V)$ as q . We know that r_v is not large enough that E_p can contain an ϵ -ball centered at q , so a line segment passing from v to q with length r_v does not extend by ϵ or more past q .

Let f be the point along the line from v to q at distance r_v from v . We seek the minimum height $h := d(p, q)$ such that $d(q, f) < \epsilon$, because at this distance an ϵ -ball would (perhaps) fit in E_p .

We also define w_v as the distance from v to q .

All the points are coplanar, so we proceed using the Pythagorean theorem. q is on the boundary of $\text{conv}(V)$ and p is outside of $\text{conv}(V)$, so we know that $\angle vqp \geq 90^\circ$, where we have equality when v is on the face of $\text{conv}(V)$ containing q . In $\triangle vqp$, since $\angle vqp \geq 90^\circ$ and $v \neq q$ we have the following.

$$h^2 \leq r_v^2 - w_v^2 \quad (6)$$

$$< (w_v + \epsilon)^2 - w_v^2 \quad (7)$$

$$= \epsilon^2 + 2w_v\epsilon \quad (8)$$

$$\implies h < \sqrt{\epsilon(\epsilon + 2w_v)} \quad (9)$$

In order to find h such that an ϵ -ball fits in E_p , we need to choose the largest bound on h for any vertex. For a fixed X we have a fixed ϵ , and the bound scales with $\sqrt{w_v}$. It is easy to show that the largest $w_v \leq m$, where $m = \text{diam}(V)$ is the maximum pairwise distance between the members of V . This leads to the final bound on h . \square

A.3 Basis Quality with high density

Proof of Theorem 2. Let $x, y \in X$ be the embedded (ordinal) positions of arbitrary points in X , let x_i, y_i denote their ordinal coordinates along axis A_i , and let x'_i, y'_i denote the true positions of their projections along the true (Euclidean) axis between the endpoints of A_i .

We first consider the scaling constant s , in order to prepare to map between positions and distances in our ordinal space and in the underlying Euclidean space. If the axis points’ projections onto the true axes are evenly-spaced, then any ϵ -ball centered on the axis will contain exactly k points and $s = 2\epsilon/k$ maps from ordinal coordinates to Euclidean coordinates, i.e., for any x on axis A_i ,

$$x'_i = sx_i = \frac{2\epsilon}{k}. \quad (10)$$

When the axis points’ projections are not evenly-spaced, we will have between one and k points in each ϵ -ball centered on the axis, so we have that

$$\frac{2\epsilon}{k} x_i \leq x'_i \leq 2\epsilon x_i. \quad (11)$$

We will choose $s = 2\epsilon$ and have that $(sx_i)/k \leq x'_i \leq sx_i$ for any x_i on axis A_i .

For the first claim, assume that for some $x \in X$ the true position of the embedding coordinate x_i is more than ϵ away from the projection x'_i . Since x_i is the closest point inside the lens with apex x formed with centers in axis endpoints, it means a ball of radius ϵ fits around the projection x'_i . Such a ball must include a point $p \in X$, but then p being inside this ϵ -ball must be in the axis set (as it is between other axis points, not above them) — contradiction. So we have that the true distance between the axis point with index x_i and x'_i is at most ϵ , and its scaled coordinate sx_i is bounded by

$$x'_i \leq sx_i + \epsilon, \quad (12)$$

$$x'_i \geq \frac{s}{k}x_i - \epsilon. \quad (13)$$

For the second claim, using the bounds from the first claim and assuming orthogonal axes, we have

$$\begin{aligned} & (s/k)^2 \cdot \widehat{\text{dist}}^2(x, y) \\ &= \sum_{i=1}^d ((s/k)|x_i - y_i|)^2 \\ &\leq \sum_{i=1}^d (|x'_i - y'_i| + 2\epsilon)^2 \\ &= \sum_{i=1}^d |x'_i - y'_i|^2 + 4\epsilon \sum_{i=1}^d |x'_i - y'_i| + 4\epsilon^2 d \\ &\leq \text{dist}^2(x, y) + 4\epsilon \sqrt{d \sum_{i=1}^d |x'_i - y'_i|^2 + 4\epsilon^2 d} \quad (*) \\ &= \text{dist}^2(x, y) + 2 \left(\text{dist}(x, y) 2\epsilon\sqrt{d} \right) + 4\epsilon^2 d \\ &= \left(\text{dist}(x, y) + 2\epsilon\sqrt{d} \right)^2 \\ &\Rightarrow s \cdot \widehat{\text{dist}}(x, y) \leq k(\text{dist}(x, y) + 2\epsilon\sqrt{d}) \end{aligned}$$

where (*) follows because the arithmetic mean is less than the square mean. To summarize, the distances between two points can be considered functions of their distances along their projections onto the axes, which are correct to within the specified tolerance.

By the same argument starting with $(1/s)\text{dist}(x, y)$ we can show $\text{dist}(x, y) \leq s \cdot \widehat{\text{dist}}(x, y) + 2\epsilon\sqrt{d}$ which concludes the proof.

A.4 Approximate Basis Quality

In this section, we provide proofs related to the quality of the approximate basis found by our algorithm, and its dimensionality estimate.

We begin with the dimensionality estimate, as this drives the upper bound for our algorithm.

Theorem 4 (dimensionality estimate). *Let $\mathcal{X} = \{x_1, x_2, \dots\}$ be an infinite sequence of i.i.d. draws from some smoothly-continuous distribution over a simply connected compact subset $V \subset \mathbb{R}^d$. Also let $X_n = \{x_1, \dots, x_n\}$ be the first n draws in \mathcal{X} , and let \hat{d}_n be the number of axes chosen by Algorithm 1 when the oracle answers consistently with distances between the points in X_n . Then $\hat{d}_n \leq d$ for all n , and as $n \rightarrow \infty, \hat{d} \rightarrow d$.*

Proof. Since V is bounded and simply connected and is fully supported by the distribution, as $n \rightarrow \infty$ the radius ϵ of the largest empty ball in $\text{conv}(V)$ converges to zero. By Theorem 1, this causes our convex hull estimates $\widehat{\text{conv}}(P) \rightarrow \text{conv}(P)$ for any subset $P \subset X_n$. For the remainder of the proof, let P and Q be the sets of axis endpoints selected by the algorithm in a given iteration of axis selection.

In some iteration of the algorithm, let A be the set of axis endpoints already chosen, and let p be the next axis endpoint selected. We choose p as the point “above” at least one point and above more points than any other candidate. It follows from Theorem 3 that since p is above some other point q , it does not lie in $\text{conv}(A)$.

If p is not affinely independent of the members of A , the algorithm terminates. This is because $\widehat{\text{conv}}(Q)$ will consist of the union of two simplexes: one with all vertices in $\widehat{\text{conv}}(P)$, and one with p as one vertex and all members but one of P as the other vertices. The algorithm rejects the new axis if the union of all possible such vertices equals $\widehat{\text{conv}}(Q)$. Since at most $d + 1$ points can be affinely independent in \mathbb{R}^d , this implies that $\hat{d}_n \leq d$ for any n .

If we have selected fewer than d axes, there will be some point p which is affinely independent of A . For sufficiently large n , any such p will be above points in $\widehat{\text{conv}}(Q)$. The union of simplexes which we compare to $\widehat{\text{conv}}(Q)$ will consist of faces of a higher-dimensional simplex. If ϵ is small enough, there will be at least one point in this simplex which is not in the union of convex hull estimates, so the algorithm will not terminate if p is selected. \square